Role of undoped cap in the scaling of thin-disk lasers

Dmitrii Kouznetsov* and Jean-François Bisson

Institute for Laser Science, University of Electro-Communications, 1-5-1 Chofu, Tokyo 182-8585, Japan
**Corresponding author: dima@ils.uec.ac.jp*

Received July 25, 2007; revised November 14, 2007; accepted December 2, 2007;
posted January 3, 2008 (Doc. ID 85644); published February 14, 2008

The optimum design of a powerful thin-disk laser implies a compromise between amplified spontaneous emission (ASE), overheating, and the round-trip losses. The power enhancement of a composite thin-disk laser made of an undoped layer bonded over a thin active layer to reduce ASE losses is estimated analytically. Scaling laws for the parameters of a disk laser are suggested for cases both with and without an anti-ASE cap. Predictions of the maximal power achievable for a given laser material are compared to the published experimental data. The anti-ASE cap allows an increase of the maximal output power proportional to the square of the logarithm of the round-trip loss. © 2008 Optical Society of America

OCIS codes: 140.3580, 140.5810.

1. INTRODUCTION

Disk lasers are under intensive research for both continuous-wave [1–7] and pulsed operation [8–11]. Such a geometry allows efficient heat sink with small wavefront distortions and is believed to be one of the most promising architectures for the high-average-power laser [2,3,5–7]. The optimum design to maximize the power limit results from an interplay between heating, round-trip losses, and amplified spontaneous emission (ASE) [12].

The anti-ASE cap, Fig. 1, was proposed to suppress the ASE and increase the maximum power [6]. The anti-ASE cap is a layer of undoped material that is index matched and bonded to the active layer underneath to form a composite structure. This cap prevents the trapping of spontaneous emission inside the active layer. The active layer remains in contact with the heat sink for efficient heat removal. The undoped layer may be several times thicker than the active layer. Its thickness may be of the order of $L/2$, and we suppose it is thick enough to neglect amplification along bouncing rays. This layer also may improve the mechanical stiffness of the disk and mitigate thermal deformations.

In this paper, we estimate the increase of the maximal output power of a disk laser due to the presence of an undoped layer used as the anti-ASE cap. In Section 2, we update the expression of the effective lifetime of the excitations of the active medium for the case of the thin disk with the ASE cap. Within our model, this lifetime is the only parameter that needs to be updated. We also define dimensionless variables useful for the analytical estimates. In Section 3, we derive the analytical estimates for the optimized parameters of the thin disk with the anti-ASE cap at a given value of background loss. The design parameters are the transverse size, the thickness of an active layers and the transmission of the output coupler. In Section 4, a comparison is made for the two cases with and without an anti-ASE cap. An analytical expression for the enhancement of the power due to the anti-ASE cap is provided. In Section 5, we verify our predictions using recent experimental data. In Section 6, we summarize our results. In Appendixes A–D, we provide the deduction of the expressions for the parameters of the optimized disk lasers.

2. EFFECTIVE LIFETIME AND DIMENSIONLESS PARAMETERS

We use a simple model [12,13] for the active material. This model indicates [12] the importance of reduction of the loss [14] for the power scaling; this loss, together with the heat generation [15,16] determines the maximal power achievable at given geometry. Usually, the loss is assumed to be considerably low [17–20]. The goal of this paper is to justify such an assumption with a simplest model. Details of the model of the active medium can be found in [12]. Following [4,12], the effective lifetime for the uncovered disk laser is estimated as $\tau=\tau_0\exp(-GL)$, where G is gain, L is transversal size, and τ_0 is the radiative lifetime of the upper level of the laser transition of a single active center (for example, a Yb^{3+}) without the ASE.

Rigorously, the estimate of the effective length of the ASE above is correct only for a photon emitted in the center of the sphere of the radius L. However, the photons emitted in the vicinity of the boundary have an opportunity to get a path of order of $2L$. At large values of gL, the exponential growth the ASE emitted toward the center of the active medium greatly compensated the lack of a path of photons emitted in the opposite direction. Therefore, just L seems to be a reasonable estimate for the effective length. The introduction of an additional adjustment parameter would require detailed consideration and would complicate analysis. A similar note refers to the case with the anti-ASE cap considered below; in both cases, our analysis gives the rough estimate. Such estimates allow

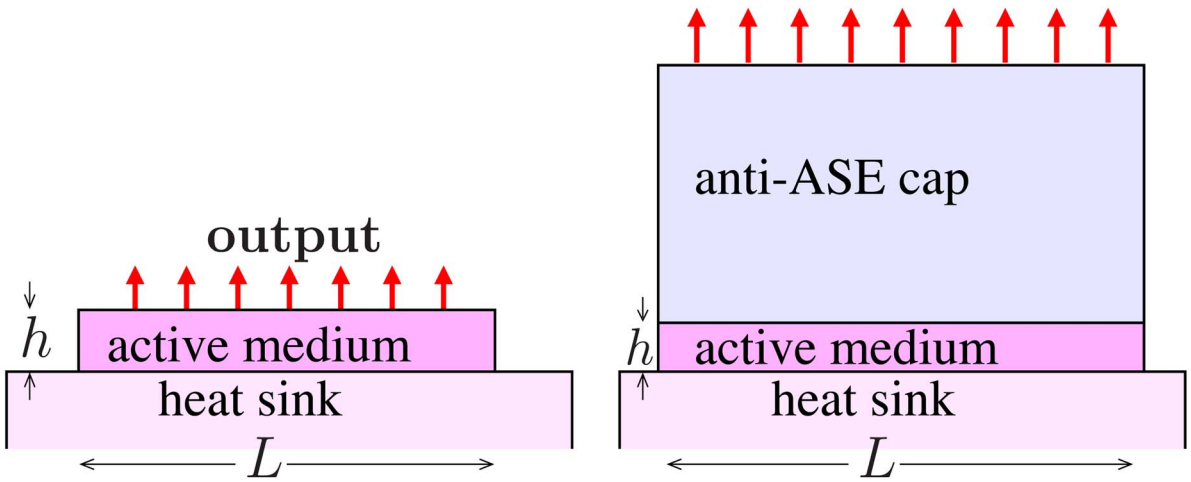

Fig. 1. (Color online) Left: uncovered thin disk laser. Right: disk with the anti-ASE cap. The external coupler is not shown in the figure.

us to reveal the scaling laws for disk lasers, but they cannot substitute the detailed numerical simulations. Through the lifetime τ the ASE affects the threshold P_{th} and therefore, the output power P_s.

In the composite disk with the anti-ASE cap, most of the spontaneous emission leaves the active medium without significant amplification. While thickness h is small compared to L (Fig. 1), only a small fraction of the ASE directed into the angle of order of h/L propagates in the plane of the disk and is strongly amplified in the gain medium. The effective decay rate $1/\tau$ can be estimated as the sum of the spontaneous emission and the ASE into angle h/L:

$$\frac{1}{\tau} = \frac{1}{\tau_o} + \frac{h}{L}\frac{\exp(GL)}{\tau_o}. \tag{1}$$

The signal output power can be estimated as [12]

$$P_s = \eta_o(1 - \beta/g)(P_p - P_{th}), \tag{2}$$

where P_p is the absorbed pump power and P_{th} is the threshold pump power, $\eta_o = \omega_s/\omega_p$ is the ratio of the frequencies of the signal and the pump and $g = 2Gh$ is round-trip gain.

The laser material can be characterized with four parameters: η_o, round-trip loss β; saturation intensity Q, and thermal loading parameter R [12]. Then, the maximization of the output power under the condition $P_p \le RL^2/h$ leads to the estimate of the limit of the power scaling of the disk lasers in terms of the key parameter $P_k = \eta_o R^2/(Q\beta^3)$. The same parameters R and Q determine also the length scale $r_o = R/Q$; optimal sizes L and h are proportional to r_o [12].

Here, we neglect the gradual drop of efficiency due to the rise of the temperature [17–20]. In this approximation, the maximum performance corresponds to $P_p = RL^2/h$ [12]. We define the power scale $P_d = R^2/Q$ and the dimensionless parameters:

$$p = P_p/P_d, \quad s = P_s/(\eta_o P_d), \quad u = GL, \quad g = 2Gh, \tag{3}$$

which are normalized pump power, normalized output power, transverse-trip gain and round-trip gain, respectively (see Table 1). These normalized powers p and s should not be confused with normalized intensities by [13]. The threshold power can be estimated with $P_{th} = g(L^2/r_o^2)(\tau_o/\tau)P_d$. The normalized output power can be estimated (Appendix A) as follows

$$s = \left(1 - \frac{\beta}{g}\right)\left(p - p^2\frac{g^3}{4u^3}\frac{\tau_o}{\tau}\right). \tag{4}$$

This expression is valid for both uncovered and composite disk lasers.

3. OPTIMIZED PARAMETERS OF THE COMPOSITE THIN-DISK LASER

In the case with the anti-ASE cap, we use the transverse-trip gain $u = GL = gL/(2h)$ for parametrization of graphics. The optimal design corresponds to the thickness h (or transverse size L) adjusted in such a way that the absorbed pump power P_p brings the medium close to overheating (or thermal fracture), determined with the thermal loading parameter R. Then, for optimized parameters, we obtain (see Appendix C)

$$\frac{(u-3)^5 e^{4u}\beta}{32u^2(6u - 2 - \beta u e^u(u-3))} = p. \tag{5}$$

The solution u of Eq. (5) versus normalized pump p is plotted in Fig. 2 with solid lines for various values of β. For comparison, at the same graph we also show the optimal u for the uncovered disk laser with a dashed horizontal line. Corresponding values of g, L, h, and s are shown in Figs. 3–5 with thick solid lines and curves. The physical (dimensional) values can be recovered using

Table 1. Example of Optimization for $P_d = 0.5$ W and $r_o = 0.1$ mm

Cap	Yes	No	Yes	No
β/%	1	1	0.1	0.1
θ/%	1	0.3	1.3	0.4
P_s/kW	225	26	435	390
L/mm	200	130	100	120
h/μm	400	460	100	200

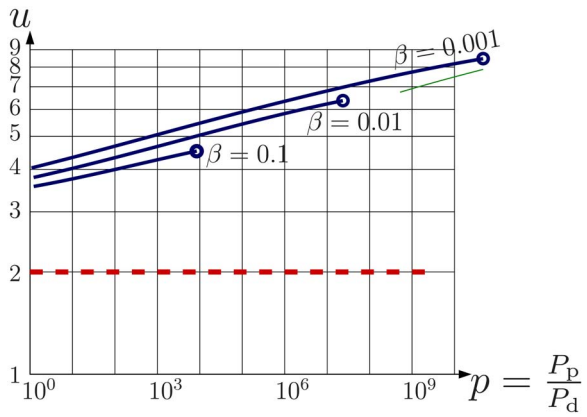

Fig. 2. (Color online) Dashed: optimal level of the transverse-trip gain $u=2$ for uncovered disk lasers. Solid: transverse-trip gain u optimized for a given pump power versus normalized pump power p at $\beta=0.1$, 0.01, and 0.001 for the disk with the anti-ASE cap by Eq. (5). Circles show the values corresponding to the maximum output power achievable at each of these β for each of the configurations (with and without the anti-ASE cap). The thin solid line shows Eq. (6) for a disk with the anti-ASE cap at $\beta=0.001$. (For Yb:YAG, $P_d \approx 0.5$ W.)

Eq. (3). Examples of such recovery are shown in Table 1.

At $\beta \ll 1$ and given p, the maximum output corresponds to

$$u \approx \frac{1}{4}\ln\frac{p}{\beta}, \quad g \approx 4\left(\frac{\beta}{p}\right)^{1/4}, \tag{6}$$

$$L \approx \frac{8r_o}{\ln\dfrac{p}{\beta}}\beta^{-1/4}p^{3/4}, \quad h \approx \frac{16r_o}{\ln\dfrac{p}{\beta}}\sqrt{\beta p}. \tag{7}$$

The asymptotic estimate for u by Eq. (6) at $\beta=0.001$ is shown in Fig. 2 with a thin solid line. It is close to the "exact" solution of Eq. (5).

The maximal output power and corresponding values of other parameters can be expressed asymptotically, using

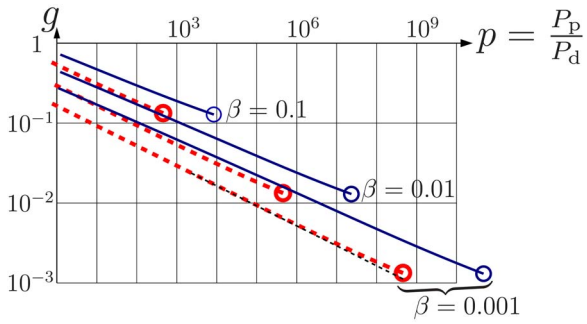

Fig. 3. (Color online) Thick dashed: optimized round trip gain g versus normalized pump power $p=P_p/P_d$ at $\beta=0.1$, 0.01, and 0.001 (uncovered disk). Solid: g versus p at the same values of β for the disk with the anti-ASE cap. The thin dashed line at the bottom represents the estimate (16) for the uncovered disk at $\beta=0.001$. Circles correspond to maxima of normalized output power at a given β. (For Yb:YAG, $P_d \approx 0.5$ W.)

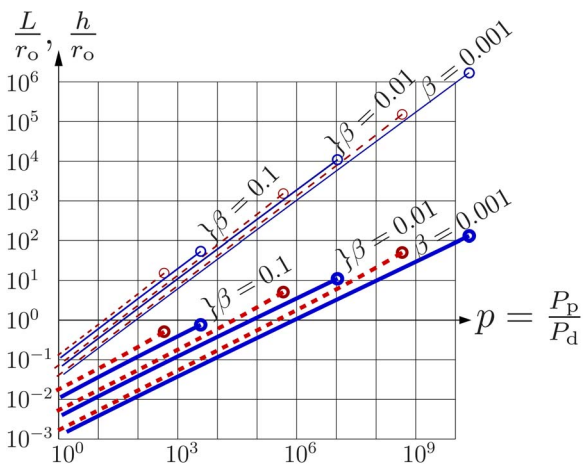

Fig. 4. (Color online) Dashed: optimized size L (thin) and thickness h (thick) versus normalized pump power p for $\beta=0.1$, 0.01, and 0.001 (uncovered disk). Solid: the same for the disk with the anti-ASE cap. (For Yb:YAG, $r_o \approx 0.1$ mm, $P_d \approx 0.5$ W.)

$$\varepsilon = \frac{1}{\ln(3/\beta)}, \tag{8}$$

as a small parameter (Appendix B):

$$u \approx \frac{1}{\varepsilon} + \frac{19}{6}\varepsilon + \mathcal{O}(\varepsilon^2), \tag{9}$$

$$g \approx \frac{4}{3}\beta\left(1 + \frac{1}{6}\varepsilon + \mathcal{O}(\varepsilon^2)\right)^{-1}, \tag{10}$$

$$L \approx \frac{r_o}{16}\left(\frac{3}{\beta\varepsilon}\right)^2\left(1 + \frac{5}{3}\varepsilon + \mathcal{O}(\varepsilon^2)\right)^{-1}, \tag{11}$$

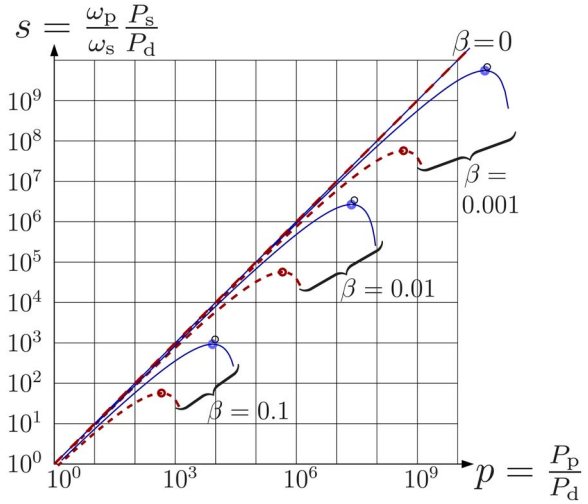

Fig. 5. (Color online) Dashed: normalized output power at optimized values of L, h (thick) versus normalized pump p at $u=2$ for $\beta=0.1$, 0.01, and 0.001 (uncovered disk); the maximal power scales up as $1/\beta^3$. Solid: similar curves for a disk with the anti-ASE cap for the same values of β. Thick circles indicates maxima of the output power. Thin circles for the disk laser with the anti-ASE cap correspond to the leading term of the asymptotic estimates (13) and (14). (For Yb:YAG, $P_d \approx 0.5$ W.)

$$h \approx \frac{r_o}{8}\left(\frac{3}{\beta}\right)\left(1+\frac{11}{3}\varepsilon+\mathcal{O}(\varepsilon^2)\right)^{-1}, \tag{12}$$

$$s \approx \left(\frac{3}{\beta}\right)^3 \frac{1}{256\varepsilon^2}(1+2\varepsilon+\mathcal{O}(\varepsilon^2))^{-1}, \tag{13}$$

$$p \approx \left(\frac{3}{\beta}\right)^3 \frac{1}{32\varepsilon^2}\left(1+\frac{3}{2}\varepsilon+\mathcal{O}(\varepsilon^2)\right)^{-1}. \tag{14}$$

The leading term of each of these expansions is shown with a thin circle in Fig. 5 for $\beta=0.1$, 0.01, and 0.001. Parameter ε depends on the loss β logarithmically, so, it is not very small. The realistic values are $0.1<\varepsilon<0.3$. For the robustness of the estimates with the first two terms of the asymptotic expansions, they are written in such a way that the partial sum remains positive, even at $\varepsilon\sim 1$.

At the maximum output power, the round–trip gain is $\sim 4/3$ of the surface loss, and the quantum efficiency does not exceed 1/8 (as in the case without the cap). The asymptotic estimate $(p_{\max,\mathrm{cap}}, s_{\max,\mathrm{cap}})$ for values $\beta=0.1$, 0.01, and 0.001 are shown in Fig. 5 with thin circles. The estimates (13) and (14) can be used as the upper bound of the power of a thin-disk laser with the anti-ASE cap.

4. COMPARISON OF PERFORMANCE BETWEEN CASES WITH AND WITHOUT CAP

In this Section, the maximal power of an uncovered disk laser (Fig. 1, left) is compared to that of the disk with the anti-ASE cap (Fig. 1, right). For an uncovered laser disk, the maximum output corresponds to $u=2$ (see [12] and Appendix B). Then, the maximization of s with respect to g gives

$$\frac{16/e^2}{3-2\beta/g}\left(\frac{\beta}{g}\right)^4 = \beta^3 p. \tag{15}$$

The solution g of this equation is plotted versus g in Fig. 3 with dashed lines for the values $\beta=0.1$, 0.01, and 0.001. (The solid lines correspond to the case with the anti-ASE cap.) As β decreases, the normalized pump power p may scale up as β^{-3}, keeping constant the right-hand side of Eq. (15). Then, the round-trip gain scales down as β, in order to keep constant the left-hand side of Eq. (15). For example, in Fig. 3, the dashed line for $\beta=0.01$ is just the same as the line for $\beta=0.001$ shifted to the left by three steps of the grid and up by one step of the grid.

In the logarithmic scale, the curves in Fig. 3 are almost straight:

$$g \approx \left(\frac{16}{3e^2}\frac{\beta}{p}\right)^{1/4} \approx 1.2\left(\frac{\beta}{p}\right)^{1/4}. \tag{16}$$

For $\beta=0.001$, this estimate is shown in Fig. 3 with a thin dashed line at the bottom. A similar scaling law takes place for the width L of the disk and its thickness h (Fig. 4):

$$L \approx \frac{r_o}{2\sqrt{e}}\left(\frac{\beta}{3}\right)^{1/4} p^{3/4} \approx 0.63 r_o \beta^{1/4} p^{3/4}, \tag{17}$$

$$h \approx \frac{r_o}{2e}\left(\frac{\beta}{3}p\right)^{1/2} \approx 0.58 r_o \beta^{1/2} p^{1/2}. \tag{18}$$

The maximum s corresponds to

$$u=2, \quad g=\frac{4}{3}\beta, \tag{19}$$

$$L=L_{\max}=\frac{r_o}{8e^2}\left(\frac{3}{\beta}\right)^2, \quad h=h_{\max}=\frac{r_o}{8e^2}\frac{3}{\beta}, \tag{20}$$

$$p=p_{\max}=\frac{1}{8e^2}\left(\frac{3}{\beta}\right)^3, \quad s=s_{\max}=\frac{1}{64e^2}\left(\frac{3}{\beta}\right)^3. \tag{21}$$

These "maximal" values are shown in Figs. 2–5 with circles. In both cases, asymptotically, the maximum output implies low efficiency (less than $\frac{1}{8}$), but in the case with the cap, the maximal power has an additional factor

$$\frac{s_{\max,\mathrm{cap}}}{s_{\max}} = \frac{e^2}{4\varepsilon^2}[1+2\varepsilon+\mathcal{O}(\varepsilon^2)]^{-1}, \tag{22}$$

where ε is defined with Eq. (8). Since the processes, neglected in the deduction, affect the output power in a similar way in both cases, we expect this estimate to be particularly reliable, especially at small values of β; taking into account only the leading term in the expansion of Eq. (22) gives reasonable estimate.

The estimates (13) and (21) of the maximal power achievable at a given β are very sensitive to β. The same expressions give robust estimates on how small β should be in order to achieve some required output power P_s. For the case without the cap [12], for a given s, the loss β should not exceed value:

$$\beta = \frac{3}{4e^{2/3}} s^{-1/3}. \tag{23}$$

For the case with the cap, the loss should not exceed

$$\beta \approx \left(\frac{3}{256s}\right)^{1/3} (\ln(256s))^{2/3}. \tag{24}$$

These estimates are shown in Fig. 6. The thin line shows $\beta=s^{1/3}$, which comes from equating $P_s=P_k$. It is the rough estimate without coefficients. It might apply to both cases with the cap and without the cap. The thick dashed curve shows the case without the undoped cap and the thick solid curve shows the case with the anti-ASE cap. The circles correspond to various experiments with disk lasers discussed in Section 6. Although the consideration above predicts the increase of the maximal power achievable in thin disk lasers due to the anti-ASE cap, the question about its application is rather generic than scientific. First, the decrease of the round-trip loss β may be less expensive than the application of the thick cap. Also, in order to suppress the bouncing rays, the thickness should be comparable to the size L of the pumped region. Then, the deformation, stress, thermal lensing, and aberrations (not considered here) may also become limiting factors. Here, we consider only the simplest model, which does not contradict the published experiments and numerical

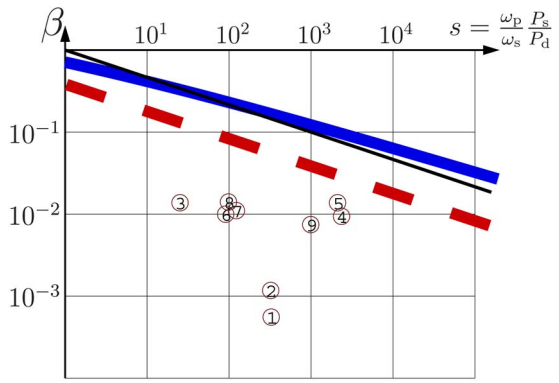

Fig. 6. (Color online) Estimates of the upper bound for the round-trip loss β required for the desired output power P_s of a thin-disk laser versus $s=(\lambda_s/\lambda_p)(P_s/P_d)$. Thin solid curve: $\beta=s^{-1/3}$, rough estimate without any coefficients. Thick dashed curve: Eq. (23) for the case without the cap. Thick solid curve: estimate (24) for the disk laser with the anti-ASE cap. Circles correspond to various lasers, and the digit in each circle indicates the row number (last column) in Table 2.

simulations. Within this model, all disk lasers with an uncovered active layer should have a background loss less than the upper bound in Eq. (23), shown with a dashed curve in Fig. 6. Lasers with the anti-ASE cap should have a loss less than the upper bound in Eq. (24), shown with the thick solid curve.

5. COMPARISON WITH EXPERIMENTS

Usually, direct measurements of the parameter β are not reported in the literature. However, β can be estimated using the slope efficiency η_s, the efficiency of the absorption of the pump η_a, and the output coupling θ. Following Eq. (1.39) of [21], we write the estimate:

$$\beta=\theta(\eta_o\eta_a/\eta_s-1). \tag{25}$$

We recover β from published results using Eq. (25) and build up Table 2. The resulting values of β and s are shown in Fig. 6. They are consistent with the limit by [12]. The significant increase of R and the reduction of Q in row 3 of Table 2 is mainly due to the reduction of the quantum defect.

In row 9, we had to guess values of θ and η_a. These parameters are not specified in [25,26]. We guessed them from other publications and using the qualitative estimate in Eq. (25). The data for the output power make us reconsider the estimate for the thermal loading parameter R; the value in Table 2 is four times that used in the estimates by [12]. Such upgrade means the increase of the maximal power achievable with this laser material. The new data [22–26] reported after the publication [12], also do not contradict the estimate (20).

The high efficiency indicates that the design of such a laser is close to optimal, therefore thickness h and transversal size L can be guessed from the scaling laws (17) and (18). In this case, $r_o=R/Q\approx 0.5$ mm, then the estimate gives $h\approx 0.3$ mm and $L\approx 8$ mm. Similar values can be obtained also from Fig. 4.

Figure 6 confirms the power limit by [12]. All the experimental circles are below the dashed curve, which shows the general limit for the uncovered disk lasers. We expect careful measurements of the quantities of Q, R, and β would allow a more precise confirmation of our upper bound for the loss β.

6. CONCLUSIONS

The performance of the uncovered disk laser and that with the anti-ASE cap were estimated analytically. The minimal model developed in [12] was used to estimate the output power in terms of size L, thickness h, round-trip gain g, and round-trip loss β. Table 3 describes the notations used in this paper. The power scaling of a thin disk laser implies the scaling up of L and h and the scaling down of the round-trip gain g. To maintain a constant efficiency, the background loss β should also be scaled down.

The scaling laws (15)–(18) and Eqs. (6) and (7) are suggested for the parameters, optimized at a given loss β and a given pump p, for both the case of the uncovered disk laser and for the disk with the anti-ASE cap. Dimensionless graphics for these parameters are shown in Figs. 2–5.

The scaling laws (19)–(21) and Eqs. (10)–(14) are suggested for the maximum output power at a given β for the same two cases. At the power scaling, the loss should be scaled down as the inverse of the cubic root of the desired output power of the uncovered disk laser, and a little bit slower for the disk with the anti-ASE cap.

The upper bounds in Eqs. (23) and (24) for the round-trip loss β in a disk laser at a given output power are sug-

Table 2. Various Lasers at the β,s Diagram

Material	h	λ_p	λ_s	R	Q	η_o	θ	η_a	η_s	P_s	Reference	P_d	β	s	Row Number
Unit	mm	nm	nm	$\frac{\text{Watt}}{\text{mm}}$	$\frac{\text{kW}}{\text{cm}^2}$	%	%	%	%	Watt		Watt	%		
3% Yb:Lu_2O_3	0.25	976	1080	8	35	90.4	0.4	95	75	33	[22]	0.15	0.06	237	1
3% Yb:Lu_2O_3	0.25	976	1080	8	35	90.4	1.6	95	80	32	[22]	0.15	0.12	231	2
3% Yb:Lu_2O_3	0.25	976	1034	14	12	94.4	5.7	95	72	26	[22]	1.51	1.51	18	3
25% Yb:LSB	0.30	974	1040	3	36	94.0	1.0	99	48	40	[23]	0.03	1.38	1702	4
20% Yb:LSB	0.30	974	1040	3	36	94.0	1.0	96	38	36	[23]	0.03	0.94	1532	5
8% Yb:YAG	0.25	941	1030	20	5	91.2	1.0	95	56	480	[5]	0.68	0.2	66	6
9% Yb:YAG	0.25	941	1030	20	5	91.2	2.0	95	60	647	[5]	0.68	0.2	89	7
10% Yb:YAG	0.20	940	1030	20	5	91.4	3.0	95	56	520	[24]	0.68	1.10	71	8
Yb:YAG	0.1	940	1030	20	5	91.4	3.0	95	70	5000	[25,26]	0.68	0.75	720	9

Table 3. Notations and Basic Formulas

ASE	Amplified spontaneous emission
G	Gain [12]
$g=2Gh$	Round-trip gain [12]
h	Thickness of the disk, Fig. 1
L	Size of the disk, Fig. 1
$P_d=R^2/Q$ ($\sim$0.5 W)	Power scale [12]
$P_k=R^2\eta_o/(Q\beta^3)$	Key parameter [12]
P_p	Absorbed pump power (A6)
P_s	Output power (A1)
$P_{th}=\frac{\hbar\omega_p L^2}{2\sigma_e\tau}g$	Threshold power (A2) [12,21]
$P_s=\eta_o(1-\beta/g)(P_p-P_{th})$	Signal power (2) (output power)
$p=P_p/P_d$	Normalized pump power (3)
$Q=\hbar\omega_p/(2\tau_o\sigma_{se})$	Saturation parameter [12]
$R=\min\begin{cases}3R_T/\eta_h\\2k\Delta T_{max}/\eta_h\end{cases}$	Thermal loading [12]
$r_o=P/Q$	Scale of size [12]
$s=P_s/(\eta_o P_d)$	Normalized output power (3)
$u=GL$	Transverse-trip gain [12]
β	Background surface loss (2)
$\varepsilon=1/\ln\frac{3}{\beta}$	Small parameter (9)
$\eta_h=1-\eta_o$	Heat generation parameter
$\eta_o=\omega_s/\omega_p$	Quantum limit of efficiency [12]
$\tau=\tau_o\exp(-GL)$	Effective lifetime [12]
$\tau=\left(\frac{1}{\tau_o}+\frac{2h}{L}\exp(-GL)\right)^{-1}$	Effective lifetime (1)
τ_o	Lifetime of the upper manifold (1)
σ_e	Emission cross section (A2)
ω_p, ω_s	Frequencies of pump and signal (A2)

gested for both cases (thick curves in Fig. 6). The improvement of the performance of an optimized thin disk laser by the anti-ASE cap can be characterized by the increase of the maximal output power achievable at a given round-trip loss β. The maximal power in the case with the anti-ASE cap has an additional factor of the order of $0.2\ln(3/\beta)^2$, according to the estimate in Eq. (22). Even with the anti-ASE cap, the reduction of the loss β remains an important condition of the power scaling of disk lasers.

The upper bound for the loss in Eq. (23) is consistent with published data. The careful measurement of β together with the other parameters in a thin-disk laser experiment at high power would be welcome.

The results above apply to both the continuous and quasi-continuous regimes of operation discussed by [12]. Similar scaling laws take place for the storage of energy in the active medium for the pulsed operation. Such an analysis should be the continuation of this work.

APPENDIX A: OUTPUT POWER IN DIMENSIONLESS VARIABLES

In this Appendix we represent the normalized output power and sizes L and h of a disk laser in terms in terms of round-trip gain g and transverse-trip u, at a given normalized pump p and given loss β. The output power [12] can be expressed with

$$P_p=\eta_o(P_s-P_{th}). \tag{A1}$$

The threshold power can be expressed as

$$P_{th}=\frac{\hbar\omega_p gL^2}{\tau\,2\sigma}=GL^2Q\frac{\tau_o}{\tau}. \tag{A2}$$

For the high efficiency, the pump power should be close to the maximal power allowed by the overheating limit. In other words, the size and thickness should be adjusted in such a way that the power P_p is close to the maximal allowed by the overheating. This gives the relation

$$RL^2/h=P_p, \tag{A3}$$

where R is the thermal loading parameter. Its value can be in the order of several watts per millimeter for Yb:YAG.

The direct maximization of expression (A1) with expression (A2) leads to complicated equations, which would allow only a numerical solution. To get the scaling laws in compact form, we use transversal gain $g=2Gh$ and round-trip gain $u=GL$ as independent parameters. Equations

$$\frac{L^2}{h}=\frac{P_p}{R},\quad \frac{L}{h}=\frac{2u}{g}, \tag{A4}$$

allow to express the sizes as follows

$$L=\frac{gP_p}{2uR},\quad h=\frac{g^2P}{4u^2R}. \tag{A5}$$

The substitution of the expression for L into expressions (A1) and (A2) gives

$$P_s=\eta_o\left(1-\frac{\beta}{g}\right)\left(P_p-\frac{P_p^2Q}{R^2}\frac{g^3}{4u^2}\frac{\tau_o}{\tau}\right). \tag{A6}$$

Using dimensionless variables p and q by Eq. (3) we obtain Eq. (4).

APPENDIX B: OPTIMIZATION OF DISK WITHOUT ANTI-AMPLIFIED SPONTANEOUS EMISSION CAP

In this Appendix we maximize Eq. (4) for the case without the cap, assuming $\tau_o/\tau=\exp(u)$. This Appendix basically follows the deduction of [12]. The only difference is that here we represent the results in a form that shows the scaling laws, which can be easily compared to those for the disk laser with the anti-ASE cap, considered in Appendix C.

The maximal output corresponds to $u=2$, then

$$s=\left(1-\frac{\beta}{g}\right)\left(p-p^2\frac{e^2}{16}g^3\right). \tag{B1}$$

The maximization with respect to g leads to the equation

$$\frac{\beta}{g^3(3g-2\beta)}=\frac{e^2}{16}p, \tag{B2}$$

which is equivalent to Eq. (15).

APPENDIX C: OPTIMIZATION OF DISK WITH ANTI-AMPLIFIED SPONTANEOUS EMISSION CAP

In this Appendix, we maximize Eq. (4) for

$$\frac{\tau_0}{\tau}=1+\frac{g}{2u}e^u, \tag{C1}$$

which corresponds to the effective lifetime by Eq. (1). Setting the derivatives of s with respect to u and g to zero, we get the equations

$$\frac{4ue^{-u}}{u-3}=g, \quad \frac{2g^4p(2e^ug+3u)}{3e^ug^4p+4g^3pu+8u^3}=\beta. \tag{C2}$$

The combination of these equations leads to Eq. (5).

APPENDIX D: MAXIMAL POWER AND THE ASYMPTOTIC ANALYSIS

Consider the case when the source of the pump can provide the pump sufficiently, then we consider dimensionless p as the optimization parameter. Equation (4) is quadratic with respect to p. This makes the first step of the analysis of the maximal power straightforward. Then, in the case without the cap, it leads to the simple representations in Eqs. (19)–(21) considered by [12].

For the case with the cap, we do not count the optimized parameters with simple representation in terms of elementary functions. As the estimates are qualitative anyway, it is worth suggesting the asymptotic expansions for the maximal output power achievable, and suggesting the corresponding estimates of the corresponding parameters of the laser. We do it in this appendix, assuming a small loss $\beta \ll 1$.

In searching the maximum of Eq. (4) with respect to p at Eq. (C1), we find

$$p=\frac{4u^3}{g^3(e^ug+2u)}, \quad s=\frac{2(g-\beta)u^3}{g^4(e^ug+2u)}. \tag{D1}$$

The maximum of s with respect to u and g corresponds to

$$\frac{4e^{-u}u}{u-3}=g, \quad \frac{2g(e^ug+3u)}{5e^ug+8u}=\beta, \tag{D2}$$

the first of these two equations is the same as in Eq. (C2). The combination gives

$$\frac{2ue^{-u}(3u-1)}{(2u-1)(u-3)}=\beta. \tag{D3}$$

This expression is used to make a parametric plot of the maximum power achievable at a given β, or a maximal β, at which a given power s still can be achieved using u as a parameter (Fig. 6). Similar parameterizations were used to plot other graphs. In this sense, the maximization of Eq. (A6) is exact. For estimates of the optimized parameters with elementary functions we assume a small loss $\beta \ll 1$. The expression (D3) can be rewritten as

$$e^u=\frac{3}{\beta}\frac{1-1/(3u)}{(1-1/(2u))(1-3/u)}, \tag{D4}$$

or

$$u=\ln\frac{3}{\beta}+\ln\left(1-\frac{1}{3u}\right)-\ln\left(1-\frac{1}{2u}\right)-\ln\left(1-\frac{3}{u}\right). \tag{D5}$$

We see, that $\varepsilon=1/\ln(3/\beta)$ can be used as the expansion parameter. Iterating, we find $u=\mathcal{O}(\varepsilon^{-1})$, then $u=\varepsilon^{-1}+\mathcal{O}(\varepsilon)$, and so on. One can calculate several terms of such asymptotic expansion, especially with the help of some software for analytical calculus, such as MAPLE or MATHEMATICA. Both were used to verify the expansions. In tracing expressions of all parameters in terms of u and replacing u with its asymptotic representation, we get estimates (9)–(14). Figure 5 shows that even the single leading term of the expansion for the maximal power gives a relatively good approximation: the thin circles (which corresponds to the leading term of the expansion) are close to the thick circles (which corresponds to the accurate numerical solution).

Within our approximation, there is no reason to get a more precise evaluation of the maximum of s as a function of p, u, g, with β as a parameter. The estimates remain qualitative anyway. However, we expect our estimates to catch the essence of the phenomenon and give the correct scaling laws for the thin disk lasers.

ACKNOWLEDGMENTS

This work was supported by the 21st Century COE program of Ministry of Education, Science and Culture of Japan. The authors are grateful to K. Ueda, J. Dong, R. Peters, O. Parriaux, and J. Li for their help and discussions.

REFERENCES

1. K. Ueda and N. Uehara, "Laser-diode-pumped solid state lasers for gravitational wave antenna," in Proc. SPIE **1837**, 336–345 (1993).
2. A. Giesen, H. Hügel, A. Voss, K. Wittig, U. Brauch, and H. Opower, "Scalable concept for diode-pumped high-power solid-state lasers," Appl. Phys. B **58**, 365–372 (1994).
3. C. Li, D. Y. Shen, J. Song, N. S. Kim, and K. Ueda, "Theoretical and experimental investigations of diode-pumped Tm: YAG laser in active mirror configuration," Opt. Rev. **6**, 439–442 (1999).
4. N. P. Barnes and B. M. Walsh, "Amplified spontaneous emission—application to Nd:YAG lasers," IEEE J. Quantum Electron. **35**, 101–109 (1999). N. P. Barnes and B. M. Walsh, "Corrections to amplified spontaneous emission—application to Nd:YAG lasers," IEEE J. Quantum Electron. **35**, 1100–1100 (1999).
5. C. Stewen, K. Contag, M. Larionov, A. Giesen, and H. Hügel, "A 1-kW CW thin disc laser," IEEE J. Sel. Top. Quantum Electron. **6**, 650–657 (2000).
6. R. J. Beach, E. C. Honea, C. Bibeau, S. Payne, A. Stephen, H. Powell, W. F. Krupke, and S. B. Sutton, "High average power scalable thin-disk laser," U.S. patent 6,347,109 (12 February 2002).
7. L. E. Zapata, R. J. Beach, E. C. Honea, and S. A. Payne, "Method for optical pumping of thin disk laser media at

high average power," U.S. patent 6,763,050 (13 July 2004).
8. K. Naito, M. Yamanaka, M. Nakatsuka, T. Kanabe, K. Mima, C. Yamanaka, and S. Nakai, "Conceptual design of a laser diode pumped solid state laser system for laser fusion reactor driver," Jpn. J. Appl. Phys., Part 1 **31**, 259–273 (1992).
9. C. D. Orth, S. A. Payne, and W. F. Krupke, "A diode pumped solid state laser driver for inertial fusion energy," Nucl. Fusion **36**, 75–116 (1996).
10. E. I. Moses and C. R. Wuest, "The national ignition facility: laser performance and first experiments," Fusion Sci. Technol. **47**, 314–322 (2005).
11. E. Innerhofer, T. Südmeyer, F. Brunner, R. Häring, A. Aschwander, R. Paschotta, C. Hönninged, M. Kumkar, and U. Keller, "60-W average power in 810-fs pulses from a thin-disk Yb:YAG laser," Opt. Lett. **28**, 367–369 (2003).
12. D. Kouznetsov, J.-F. Bisson, J. Dong, and K. Ueda, "Surface loss limit of the power scaling of a thin disk laser," J. Opt. Soc. Am. B **23**, 1074–1082 (2006).
13. D. Kouznetsov, J.-F. Bisson, K. Takaichi, and K. Ueda, "High-power single mode solid state laser with a short unstable cavity," J. Opt. Soc. Am. B **22**, 1605–1619 (2005).
14. N. Uehara, A. Ueda, K. Ueda, H. Sekiguchi, T. Mitake, K. Nakamura, N. Kitajima, and I. Kataoka, "Ultralow-loss mirror of the parts-in-10^6 level at 1064 nm," Opt. Lett. **20**, 530–532 (1995).
15. W. F. Krupke, M. D. Shinn, J. E. Marion, J. A. Caird, and S. E. Stokowski, "Spectroscopic, optical, and thermomechanical properties of neodymium- and chromium-doped gadolinium scandium gallium garnet," J. Opt. Soc. Am. B **3**, 102–114 (1986).
16. T. Y. Fan, "Heat generation in Nd:YAG and Yb:YAG," IEEE J. Quantum Electron. **29**, 1457–1459 (1993).
17. T. Kasamatsu, H. Sekita, and Y. Kuwano, "Temperature dependence and optimization of 970 nm diode-pumped Yb:YAG and Yb:Lu:AG lasers," Appl. Opt. **38**, 5149–5153 (1999).
18. J. Lu, J. Lu, T. Murai, K. Takaichi, T. Uematsu, K. Ueda, H. Yagi, T. Yanagitani, and A. A. Kaminskii, "$Nd^{3+}:Y_2O_3$ ceramic laser," Jpn. J. Appl. Phys., Part 1 **40**, L1277–L1279 (2001).
19. J. Kawanaka, "We consider HR-coating on the backside, and AR-coating or Brewster-angled incidence on the front side; the scattering is considerably low" (personal communication, 2005).
20. Q. Liu, M. L. Gong, Y. Y. Pan, and C. Li, "Edge-pumped composite thin-disk Yb:YAG/YAG laser: design and power scaling," Acta Phys. Sin. **53**, 2159–2164 (2004).
21. B. Henderson and R. H. Bartram, *Crystal-Field Engineering of Solid-State Materials* (Cambridge U. Press, 2000).
22. R. Peters, C. Kränkel, K. Petermann, and G. Huber, "Broadly tunable high-power $Yb:Lu_2O_3$ thin disk laser with 80% slope efficiency," Opt. Express **15**, 7075–7082 (2007).
23. P. Kränkel, J. Johannsen, R. Peters, K. Peterman, and G. Huber, "Continuous wave high power laser operation and tunability of $Yb:LaSc_3(BO_3)_4$ in thin disk configuration," Appl. Phys. B **87**, 217–220 (2007).
24. M. Tsunekane and T. Taira, "High-power operation of diode edge-pumped, composite all-ceramic $Yb:Y_3Al_5O_{12}$ microchip laser," Appl. Phys. Lett. **90**, 121101 (2007).
25. A. Giesen, L. Speiser, R. Peters, C. Kränkel, and K. Peterman, "Thin-disk lasers come of age," Photonics Spectra **41**, 52–58 (2007).
26. A. Giesen and J. Speiser, "Fifteen years of work on thin-disk lasers: results and scaling laws," IEEE J. Sel. Top. Quantum Electron. **13**, 598–609 (2007).